Matter and Radiation at Extremes | RESEARCH ARTICLE | scitation.org/journal/mre

Focal-shape effects on the efficiency of the tunnel-ionization probe for extreme laser intensities

Cite as: Matter Radiat. Extremes 5, 044401 (2020); doi: 10.1063/5.0005380
Submitted: 25 February 2020 • Accepted: 16 June 2020 •
Published Online: 17 July 2020

M. F. Ciappina,[1,2] E. E. Peganov,[3,4] and S. V. Popruzhenko[4,a)]

AFFILIATIONS

[1] Institute of Physics of the ASCR, ELI-Beamlines Project, Na Slovance 2, 182 21 Prague, Czech Republic
[2] ICFO—Institut de Ciencies Fotoniques, Barcelona Institute of Science and Technology, Av. Carl Friedrich Gauss 3, 08860 Castelldefels (Barcelona), Spain
[3] National Research Nuclear University MEPhI, Kashirskoe Ave. 31, 115409 Moscow, Russia
[4] Prokhorov General Physics Institute of the Russian Academy of Sciences, Vavilov Str. 38, 119991 Moscow, Russia

Note: This paper is part of the Special Issue on Atomic and Molecular Physics for Controlled Fusion and Astrophysics.
[a)]**Author to whom correspondence should be addressed:** sergey.popruzhenko@gmail.com

ABSTRACT

We examine the effect of laser focusing on the effectiveness of a recently discussed scheme [M. F. Ciappina *et al.*, Phys. Rev. A **99**, 043405 (2019) and M. F. Ciappina and S. V. Popruzhenko, Laser Phys. Lett. **17**, 025301 (2020)] for *in situ* determination of ultrahigh intensities of electromagnetic radiation delivered by multi-petawatt laser facilities. Using two model intensity distributions in the focus of a laser beam, we show how the resulting yields of highly charged ions generated in the process of multiple sequential tunneling of electrons from atoms depend on the shapes of these distributions. Our findings lead to the conclusion that an accurate extraction of the peak laser intensity can be made either in the near-threshold regime, when the production of the highest charge state happens only in a small part of the laser focus close to the point where the intensity is maximal or through the determination of the points where the ion yields of close charges become equal. We show that for realistic parameters of the gas target, the number of ions generated in the central part of the focus in the threshold regime should be sufficient for a reliable measurement with highly sensitive time-of-flight detectors. Although the positions of the intersection points generally depend on the focal shape, they can be used to localize the peak intensity value in certain intervals. Finally, the slope of the intensity-dependent ion yields is shown to be robust with respect to both the focal spot size and the spatial distribution of the laser intensity in the focus. When these slopes can be measured, they will provide the most accurate determination of the peak intensity value within the considered tunnel ionization scheme. In addition to this analysis, we discuss the method in comparison with other recently proposed approaches for direct measurement of extreme laser intensities.

I. INTRODUCTION

The interaction of high-power electromagnetic radiation with different forms of matter, including free electrons, atoms, molecules, solids, and plasmas, has been an important topic of experimental and theoretical research for more than 50 years, since the early days of laser physics. For the fundamental phenomena that can potentially be observed in such interactions, the strengths of the electric and magnetic fields of laser radiation are crucial parameters determining the interaction scenario and indeed the very possibility of experimentally observing various effects. Progress in the development and application of high-power laser sources had led to a gradual growth in the maximum available field strengths. This has already made it possible to experimentally explore the nonlinear quantum dynamics of atomic, molecular, and solid state systems subjected to intense laser radiation, the physics of relativistic and ultrarelativistic electron plasmas, and relativistic nonlinear optics (see Refs. 1–6 and references therein for an overview of these research fields). Currently, electromagnetic fields of peak strength $E_0 \approx 10^{12}$ V/cm can be achieved in infrared and optical femtosecond pulses generated by multi-terawatt (TW) and petawatt (PW) laser systems. For linearly polarized radiation, such an electric field corresponds to an intensity

$$\mathcal{I} = \frac{cE_0^2}{8\pi} \approx 10^{21}\ \mathrm{W/cm^2}. \quad (1)$$

Although individual reports of even higher intensities of $\approx 10^{22}$ W/cm^2 have been published,[7–10] there have been no independent unambiguous confirmations.

Several laser facilities with multi-PW power have recently been commissioned and should start operating in the near future. An incomplete list of such laser sources includes Apollon in France,[11] APRI[12] in South Korea, CAEP[13] and SULF[14] in China, and ELI in the Czech Republic, Hungary, and Romania.[15,16] These new facilities are expected to start experimental campaigns in a couple of years, forming a network of 10-PW class laser sources. Projects with even more powerful, sub-exawatt lasers are currently under development.[17] These new technical achievements will open the door to experiments with electromagnetic fields of intensity 10^{22} W/cm^2–10^{24} W/cm^2, allowing physicists to enter so-far unexplored regimes of laser–matter interaction, including radiation-dominated dynamics of isolated charges and plasmas, laser initiation of cascades of elementary particles, excitation of extremely strong magnetic fields, and a plethora of laboratory astrophysics phenomena.[4–6]

In view of these expectations, the problem of precise characterization of the electromagnetic field distribution in a laser focus, and in particular the determination of the value of the peak intensity, becomes of great practical importance. At high radiation power, direct measurement of the intensity distribution using cameras is clearly impossible, while extrapolation of results recorded in the low-power regime is questionable and can only be considered as an indirect, and generally uncontrollable, estimation method. Thus, it is commonly accepted that reliable methods for laser focus characterization in the high-power regime should employ observation of effects whose magnitude is highly sensitive to the parameters of the laser pulse.

Several proposals for experimental characterization of a laser focus at extreme intensities have been discussed. The list of currently examined methods for *in situ* intensity measurement includes diagnostics based on multiple tunneling ionization of heavy atoms,[18–25] on scattering of laser light by electrons,[26–28] and on ponderomotive scattering of electrons, protons, or even heavy ions in the laser focus.[28–31] In this paper, we continue our analysis of atomic diagnostics based on the observation of tunneling ionization of multi-electron atoms in a laser focus.[23–25] The idea of the method is to employ the highly nonlinear dependence of the probability of tunneling ionization both on the amplitude of the applied electromagnetic field and on the ionization potential of atomic levels. This nonlinearity appears in the form of the celebrated tunneling exponent[32] and allows us to estimate the peak intensity by knowing the highest charge state produced in the laser focus filled by a low-density gas of high-Z atoms, with Z being the charge of the nucleus. Noble gases commonly used in strong-field experiments are particularly convenient for such measurements. For each charge state, there is a well-defined value of the threshold intensity required to produce a noticeable amount of the respective ions. In particular, observation of bare ions of Ar^{18+}, Kr^{36+}, and Xe^{54+} would allow proof that intensities $\approx 3 \times 10^{21}$ W/cm^2, 3×10^{23} W/cm^2, and 2×10^{24} W/cm^2, respectively, had been achieved.[23,25] The idea of atomic diagnostics based on multiple ionization of noble gases was proposed and experimentally verified in Refs. 18–22 for intensities in the range of 10^{16} W/cm^2–10^{19} W/cm^2.

In our earlier publications,[23–25] the method of atomic diagnostics was theoretically examined with emphasis on the measurement of ultrahigh intensities $\mathcal{I} > 10^{21}$ W/cm^2. A brief summary of the results obtained can be found in Sec. II. The aim of the present paper is to consider the effect of the focal distribution of laser intensity on the ionic signal that can be measured by a time-of-flight (TOF) detector of ions. As was demonstrated in Ref. 25, the intensity dependence of the ionic signal results from an interplay between the dependence of the tunneling exponent on the laser field strength and the volume effect determined by the shape of the laser focus. Here, we present a more detailed consideration of this problem by exploring two focus shapes, including an exact solution to the Maxwell equations that describes a tightly focused static laser beam.[33] Our results deliver three important messages:

(a) If a TOF detector is sensitive enough to register a few dozens of highly charged ions generated in the central part of the focus, and the gas density in the jet and the beam focal diameter can be accurately controlled, this will allow determination of the peak value of the intensity with a reasonable accuracy independently of the particular form of the intensity distribution within the focal spot.
(b) Simultaneous observation of intersections between the intensity-dependent yield curves would allow extraction of the peak value of intensity independently of the result obtained in (a) and of the value of the concentration in the atomic jet.
(c) If the laser is stable enough to provide subsequent shots at gradually growing values of the pulse energy, then measurement of the ionic yield slopes could deliver the most precise information on the peak intensity, essentially independently of the focal spot size, initial atomic concentration, and focal intensity distribution.

The rest of the paper is organized as follows. In Sec. II, we give a brief overview of the recently discussed methods for *in situ* measurement of the peak laser intensity and its distribution in the focal spot. In particular, Sec. II C presents a concise description of atomic diagnostics based on observations of tunneling ionization of multi-electron atoms, including results reported in our previous publications.[23–25] In Sec. III, we describe two models of the laser focus that are later used to examine the focal-averaging effect. The results of this examination are reported in Sec. IV. Section V presents our conclusions in brief. Atomic units are used throughout unless otherwise stated.

II. PROPOSALS FOR *IN SITU* MEASUREMENT OF LASER INTENSITY

The task of measuring the peak value of laser intensity or its distribution in space imposes several significant requirements on the effects that can potentially be used. To avoid the generation of an additional field comparable to that of the laser wave, the target has to be sufficiently rarefied, which implies the use of gases at low pressure or electron or ion beams of low density. The crucial requirement imposed on any potential method for determination of the peak intensity value is that the observed effect should be sensitive to the local values of the electric and magnetic fields. As an example, for an atom in a low-pressure gas environment, the probability of its ionization is determined by the electromagnetic fields in the close vicinity of the atom. By contrast, the momentum distributions of photoelectrons produced by ionization of this atom are formed not only by the dynamics of the ionization event, but also by the motion of the photoelectrons from the atom to the detector through the laser focus, where they experience ponderomotive scattering. Thus, for the realistic case of a large number of atoms distributed in the laser focus, it

is hardly possible to extract unambiguous information on the intensity value from the photoelectron spectra.

The requirements of locality and low target density leave only a few effects to be considered as potential candidates for an *in situ* intensity probe. So far, tunnel ionization,[18,20,22,23] nonlinear Thomson scattering (NTS),[26–28] and ponderomotive scattering of electrons[28,29] and protons[30] have been examined with the aim of reaching this objective. Below, we briefly describe these effects, giving a more detailed account of the method based on tunnel ionization.

A. Thomson scattering

In the field of an intense electromagnetic wave, the classical motion of a charged particle becomes nonlinear. The nonlinearity is governed by the relativistically invariant dimensionless intensity parameter

$$a_0 = \frac{zE_0}{mc\omega}, \tag{2}$$

with z and m being the particle charge number and mass, in atomic units $z = m = 1$ for the electron. The onset of nonlinear and relativistic effects, $a_0 = 1$, corresponds to an intensity $\mathcal{I} \approx 1.4\times10^{18}$ W/cm^2 for an electron in a field with linear polarization and $\lambda = 1$ μm. Thus, for the intensities of interest, the electron motion is highly nonlinear and ultrarelativistic. The former results in emission of high harmonics of the laser frequency, and the latter makes the instantaneous angular distribution of emitted radiation strongly peaked along the instantaneous velocity vector. Radiation by a charged particle in the field of an intense electromagnetic wave is known as nonlinear Thomson scattering (NTS), the classical limit ($\hbar \to 0$) of nonlinear Compton scattering.[34,35] A detailed account of the theory of NTS can be found in Ref. 36. The angular distributions and spectra of the emitted radiation depend in particular on the laser field amplitude, which makes them of potential use for determining the peak intensity value.

In Ref. 26, it was proposed to measure the intensity via the angular offset in the distribution of radiation emitted by an ultrarelativistic electron counterpropagating to the laser pulse under examination. It was shown that an intensity $\approx 4 \times 10^{22}$ W/cm^2 can be inferred with ≈10% accuracy if an electron beam of energy $\epsilon_0 = 23$ MeV with a narrow ≈5% energy spread collides with the laser pulse, and the angular distribution offset is measured with accuracy ≈1%. The peak intensity can be inferred with greater credibility when both radiation of an electron beam and its scattering are simultaneously characterized. This approach was examined in Ref. 28. It was shown there that a highly accurate measurement becomes possible when an electron beam with a gamma factor $\gamma \gg a_0$ and a width $b \ll w_0$, where w_0 is the laser focal waist, collides with a counterpropagating laser pulse. Simultaneous measurement of the radiation angular variance and of the mean electron energies before and after the interaction allows the peak value of a_0 to be extracted with an accuracy ≈10%. In the field amplitude range $5 < a_0 < 150$, where the upper limit corresponds to an intensity $\approx 5 \times 10^{22}$ W/cm^2, this scheme has also been shown to be practically insensitive to the model chosen for the description of the radiation reaction effect. The schemes in Refs. 26 and 28 potentially provide highly accurate intensity measurements. However, they need to use an electron beam of controllable high quality, which may complicate experimental realizations.

In a monochromatic field, the frequency ω_s of the sth harmonic emitted by an electron generally depends on the angle θ between the wave vectors of the photon and electromagnetic wave and on the intensity parameter from Eq. (2):[36]

$$\omega_s = \omega_s(a_0, \theta, \psi_0). \tag{3}$$

In the special reference frame where the electron is on average at rest, $\omega_{s0} = s\omega_0$, with ω_0 being the laser frequency there. Equation (3) then results from a Lorentz transformation to the laboratory frame. Here, the variable ψ_0 denotes the initial condition for the electron's motion, which essentially specifies the character of the trajectory in the laboratory frame. By knowing this initial condition and measuring the frequency ω_s at fixed emission angle θ, one can extract the value of a_0 and therefore that of $\mathcal{I} = c^3\omega^2 a_0^2/8\pi$.

This procedure was demonstrated in a recent experiment,[27] where a peak intensity value $\approx 10^{18}$ W/cm^2 was estimated from measurement of the second-harmonic shift. NTS of laser radiation proceeded on electrons generated in the focus owing to strong-field ionization of molecular nitrogen at a backing pressure $\approx 10^{-3}$ mbar. Thomson radiation was then separated from that resulting from recombination, and the second-harmonic frequency profile in the direction perpendicular to that of laser beam propagation was recorded. The measured value of the intensity appeared to be in fair agreement with estimates of the peak intensity extracted from images of the focal area, obtained at reduced laser power.

The main drawback of this method stems from the dependence of the frequency shift in Eq. (3) on the initial condition. In Ref. 27, where the electron plasma was created by tunneling ionization on the leading edge of the laser pulse, a particular form of Eq. (3) was used that corresponded to the electron being initially at rest. However, with increasing peak intensity, and therefore increasing ionization potentials of ionic species, this assumption will become less relevant, because ionization events may also occur a considerably time after the leading edge of the pulse has interacted with the gas. As a consequence, the relation in Eq. (3) exhibits a significant dependence on the time instant, within the laser pulse duration, at which the electron was released. This will make the procedure of intensity extraction from the spectra less unambiguous than it was in Ref. 27. Another restriction of this method results from the smallness of the focal spot size and the short pulse duration required to reach extreme intensities of electromagnetic radiation: in a nonmonochromatic field, the broadening of NTS spectra can considerably hinder determination of the intensity-induced shift. This is precisely the case for intensities 10^{23} W/cm^2 and higher, which can only be reached through tight focusing with a waist of a few micrometers. An electron will then move in a field whose spatial inhomogeneity scale is comparable to the laser wavelength. Complications in the intensity extraction algorithm that become more serious with increasing intensity are discussed in Ref. 27. Finally, at ultrahigh intensities $>10^{25}$ W/cm^2, NTS from protons[27] can be used for the same purpose.

B. Scattering of electrons and ions on the laser beam

The intensity distribution in a laser focus can also be probed through scattering of charged particles. This approach has been theoretically examined for electrons and protons (see, e.g., the recent Refs. 29, 30, and 37, and references therein). Scattering of charged particles on a laser focus in the limit of low density, when the self-field

of the beam has no effect on the particle dynamics and radiation, have been widely considered, starting from the pioneering work by Kibble.[38] A detailed account of the theory of relativistic ponderomotive scattering can be found in Refs. 33 and 39. Generally, there is no doubt that momentum distributions of electrons or protons after their interaction with a laser beam carry complete information on the peak intensity value and on the intensity distribution in space and time. The challenge is to find a suitable setup where the inverse problem of extraction of these values from the spectra can be reliably solved. Scattering of electron bunches on a laser focus can give information on the peak intensity value through measurement of the maximum deflection angle of the electrons.[29] This approach suffers a serious drawback, however: a certain spatial profile of the laser has to be assumed to calculate the angle. Besides, additional constraints are imposed on the parameters of the electron beam, introducing extra difficulties into the experimental scheme and increasing uncertainties in the interpretation of results.

Reference 30 presented a theoretical examination of laser pulse diagnostics based on the detection of momentum distributions of protons produced in ionization of a rarefied hydrogen target and ponderomotively accelerated from the laser focus. In the nonrelativistic domain of intensities for protons, $\mathcal{I} \le 10^{24}$ W/cm^2, the method was shown to reliably determine the peak value of intensity via the cutoff position in the energy spectra. Moreover, the focal spot size was shown to be related to the angular width of the proton spectra. A recent paper[31] examined laser acceleration of highly charged ions, up to Kr^{36+}, produced through tunneling ionization. It was shown that at intensities $\approx 10^{23}$ W/cm^2 and for a tightly focused pulse with $1/e^2$ diameter ≈ 3 μm, the ponderomotive force strongly modifies the energy spectra, even for such heavy ions. A sharp cutoff of these spectra observed in the simulation (see Figs. 2 and 3 in Ref. 31) can also be used as a measure of the laser intensity.

C. Tunneling ionization of heavy atoms

Nonlinear ionization of atoms or ions and related phenomena have been used as a probe of laser intensity for several decades. At moderate intensities $\mathcal{I} \approx 10^{13}$ W/cm^2–10^{15} W/cm^2, single-electron above-threshold ionization (ATI) and the generation of high-order harmonics [high-harmonic generation (HHG)] are routinely observed processes. The theory of ATI and HHG has been advanced to the level of quantitative accuracy (see Refs. 1, 2, and 40–42, and references therein for reviews), which allows extraction of the peak laser intensity from the position of the cutoff in HHG and high-energy ATI spectra or other characteristic features of photoelectron momentum distributions (for the latter, see, e.g., Ref. 43) with ~10% accuracy. Measurements of photoelectron spectra have also been shown to allow full characterization of laser pulses, including their carrier envelope phase.[44] In determinations of the peak intensity, accuracies up to 1% can be achieved by comparing experimental photoelectron yields from atomic hydrogen with predictions from exact numerical solutions of the three-dimensional time-dependent Schrödinger equation.[45] At higher intensities, HHG and high-order ATI vanish, and photoelectron distributions become affected by ponderomotive scattering, as discussed above. The degree of ionization of an atomic species then becomes the simplest measure of the peak intensity. The fundamental advantage of nonlinear ionization as a probe of laser intensity stems from the relative physical simplicity of the process: the higher the intensity, the smaller are the effects of electron–electron correlations and nonadiabaticity, owing to the smallness of the Keldysh parameter[46]

$$\gamma = \frac{\sqrt{2I_p}\omega}{E_0} \sim \mathcal{I}^{-1/2}, \tag{4}$$

where I_p is the ionization potential of the bound state. For intensities $\mathcal{I} > 10^{15}$ W/cm^2 and wavelengths in the infrared range, $\lambda \approx 1$ μm, ionization proceeds in the regime $\gamma < 1$, known as optical tunneling. In the intensity domain $\mathcal{I} > 10^{20}$ W/cm^2 of interest here, $\gamma \ll 1$ and the electromagnetic field of the laser wave can be considered static during the tunneling event, which makes formulas for the probability of quasistatic tunneling [known as Perelomov–Popov–Terentiev (PPT) rates[47,48]] quantitatively applicable to the description of multiple sequential ionization of heavy atoms. The validity of these formulas at relativistic intensities has been proven by measurements of the intensity dependence of ion yields recorded in ionization of noble gases at $\mathcal{I} \approx 10^{19}$ W/cm^2.[18–21] These measurements aimed to check the accuracy of the PPT tunneling formulas, but at the same time they offered a way to precisely measure high laser intensities using multiple tunneling ionization of heavy atoms. In a subsequent publication,[22] the method of *in situ* peak intensity measurement was experimentally verified at the Sandia Z PW laser facility. In Ref. 22, the basic principle of the method was clearly formulated as "Detection of (the) highest ionization charge state of a species and nondetection of (the) next highest charge state essentially impose a lower and an upper bound on peak intensity, when the measurement is performed with a highly efficient detection system." It was demonstrated that a sufficient number of multiply charged ions can be detected in the single-shot regime, which is of particular importance for laser sources of ultrahigh power operating at low repetition rates.

The scheme of Refs. 18–22 was examined in Refs. 23–25 with the aim of adapting it for the diagnostics of extremely intense laser pulses in the future multi-PW laser facilities. These studies revealed the following:

- Tunneling proceeds in the nonrelativistic regime up to intensities $\mathcal{I} \approx 10^{26}$ W/cm^2, so that nonrelativistic PPT rates can be safely used for calculations.[23] This statement must not be confused with the fact that *after* the tunneling, the electron motion in such intense fields quickly becomes ultrarelativistic. This relativistic stage affects only the photoelectron distributions and not the ionic yields.
- Although, for heavy atoms and high-charge ionic states, the system of rate equations describing ionization cascades that develop from a neutral atom appear extremely cumbersome, it was shown that owing to the highly nonlinear dependence of the tunneling ionization rates on the values of ionization potentials and on the laser field amplitude, this system can be reduced to a great extent to one containing only about a dozen equations.[23] This allows considerable speeding up of numerical calculations.
- The exponential dependence of the tunneling rates on the values of the ionization potential I_p and field amplitude E_0 allows the derivation of a simple and yet reliable estimate for the threshold intensity at which a given level is quickly ionized. In terms of the laser field amplitude, this condition reads[23] $E_* \approx 0.05\,(2I_p)^{3/2}$ and can be used to select a suitable target for probing a certain intensity interval.

- There is a danger that ionic states chosen for intensity diagnostics will not be fully saturated in the tunneling regime of ionization, but, with a further increase of intensity, the ionization process will partially proceed in the barrier suppression regime. Barrier suppression ionization (BSI) is not covered by such a quantitatively precise theory as tunneling ionization (for an overview of approximate methods for the description of BSI, see Refs. 49–51 and references there), and therefore entering the BSI regime can considerably decrease the accuracy of the method. To avoid this pitfall, ionization of H- and He-like ions should preferably be used, which imposes an additional constraint on the atomic constituents of the target.[25]
- Finally, the focal volume effect was briefly examined in Ref. 25. It was shown that the focal-integrated ionic signal exhibits two characteristic features that can be used for determination of the peak intensity value and, to some extent, of the focal shape. These are (a) the position of a steep part of the intensity-dependent yield, where the number of ions per laser shot increases by two orders of magnitude while the peak intensity grows by 30%–50%, and (b) the intersection point of the numbers of two neighboring ionic states: $N(A^{n+}) \approx N(A^{(n+1)+})$.

In Sec. III, we present a further analysis of the effect of focal volume on the accuracy of intensity measurement.

III. CALCULATION OF THE FOCAL-AVERAGED IONIC SIGNAL

In the nonrelativistic regime of tunneling, which correctly describes production of ionic states at intensities up to ~10^{26} W/cm^2,[23] ionization rates depend only on the absolute value of the electric field $E(t)$, while the magnetic field has no significant effect. In a focused laser pulse, the electric and magnetic field vectors are no longer orthogonal and equal in absolute value. This means that an atomic diagnostics based on the ionization mechanism will measure not the absolute value of the Poynting vector, but the electric field amplitude E_0. To avoid confusion, below we refer to the value given by Eq. (1) as the *effective* intensity.

For a given time dependence of the electric field $\mathbf{E}(\mathbf{r}, t)$, the populations $c_k(\mathbf{r}, t)$ of ionic states A^{k+} can be found by solving numerically the system of rate equations with time-dependent coefficients expressed as linear combinations of tunneling ionization rates. These systems for argon, krypton, and xenon, appropriately truncated from the side of small k, were formulated and examined in Ref. 23. When the coefficients c_k are computed, their values at the end of the laser pulse, $t = T$, give the distribution $C_k(\mathbf{r}) \equiv c_k(\mathbf{r}, T)$ over the charge states A^{k+} at a fixed point in space. The number of ions of charge $0 \le k \le Z$ produced in the focal volume is then given by the integral

$$N(A^{k+}) = n_0 \int C_k(\mathbf{r})\, d^3 r, \tag{5}$$

with n_0 being the initial concentration of neutral atoms. In the coefficients C_k, the $\mathbf{r}$ dependence enters via that of the electric field amplitude or, equivalently, the effective intensity [Eq. (1)], so that C_k can be considered as functions of the latter. These functions were numerically calculated in Ref. 23 for the pulse time envelope $\sin^2(\pi t/T)$, with a full duration $T = 33$ fs, corresponding to 10 periods at $\lambda = 1$ μm. The intensity intervals were chosen to be 10^{19} W/cm^2–10^{22} W/cm^2 for Ar^{14+}, . . ., Ar^{18+} and Kr^{26+}, . . ., Kr^{34+} and 10^{21} W/cm^2–5×10^{24} W/cm^2 for Xe^{50+}, . . ., Xe^{54+}. Ionization potentials were taken from Refs. 52–54.

To examine the potential influence of the focal distribution on the ion yield, including its dependence on the peak intensity value $\mathcal{I}_m$, we consider two model pulse shapes, namely, the simplest TEM_{00} Gaussian beam and an exact solution to the Maxwell equations for a stationary focused beam found in Ref. 33.

A. Gaussian beam

For the TEM_{00} Gaussian beam, the following intensity distribution results:

$$\mathcal{I}(x, y, z) = \frac{\mathcal{I}_m}{1 + z^2/z_R^2} \exp\left[-\frac{2(x^2 + y^2)}{w_0^2(1 + z^2/z_R^2)}\right], \tag{6}$$

where w_0 is the beam waist and $z_R = \pi w_0^2/\lambda$ is the Rayleigh length. For numerical calculations, we take $w_0 = 3$ μm, and so for $\lambda = 1$ μm, $z_R \approx 28.3$ μm, the FWHM focal spot diameter $d_0 = \sqrt{2\ln 2}\, w_0 \approx 3.5$ μm and the beam angular divergence $\theta = \arctan(\lambda/\pi w_0) \approx 0.105$. At these values of the parameters, the value of d_0 is close to that reported in Ref. 10 for the 10-PW SULF laser facility with its focusing ability improved by optimizing the wavefront aberrations. The ion yield $N(A^{k+})$ is most sensitive to the value of $\mathcal{I}_m$ near the ionization threshold of the $(k-1)$th charge state, where $\mathcal{I}_m \approx \mathcal{I}_*(A^{k+})$.[23,25] In this domain, the ions are predominantly generated in close proximity to the field maximum, where the distribution can be approximated by the parabolic expansion in Eq. (6). Then, the volume with intensities $\mathcal{I}_0 \le \mathcal{I} \le \mathcal{I}_m$ grows as

$$V \approx \frac{2\pi}{3} \frac{w_0^3}{\theta} \left(1 - \frac{\mathcal{I}_0}{\mathcal{I}_m}\right)^{3/2}. \tag{7}$$

B. Narozhny–Fofanov beam

We will compare results obtained for the beam in Eq. (6) with those for another focused beam, which is an exact stationary solution to the Maxwell equations found by Narozhny and Fofanov[33] (referred below as the NF beam). This solution describes a family of stationary (monochromatic) focused beams that are superpositions of plane waves with wave vectors lying inside a cone with an aperture angle 2Δ. The wave vectors $\mathbf{k}$ are uniformly distributed in a polar angle with respect to the beam axis z and may have a nontrivial distribution in angle α between the projection of $\mathbf{k}$ on the plane perpendicular to the z axis and the x axis; see Fig. 1 for an illustration. This solution, given by Eqs. (5)–(14) of Ref. 33, can describe different polarizations defined in the limit $\Delta \to 0$ corresponding to the plane wave. For our purposes, we use a particular solution corresponding to a beam with asymptotically linear polarization along the x axis and with the transverse electric field such that $E_z = 0$ everywhere. This solution can be expressed in the form

$$\mathbf{E}(\mathbf{r}, t) = \frac{iE_0\Delta^2}{2\pi(1 - \cos\Delta)} \exp\left[-i\omega\left(t - \frac{z}{c}\right)\right] \times \int_{-\pi}^{+\pi} d\alpha\, (\sin^2\alpha\, \mathbf{e}_x - \sin\alpha\cos\alpha\, \mathbf{e}_y) G(\nu, \chi, \Delta), \tag{8}$$

where

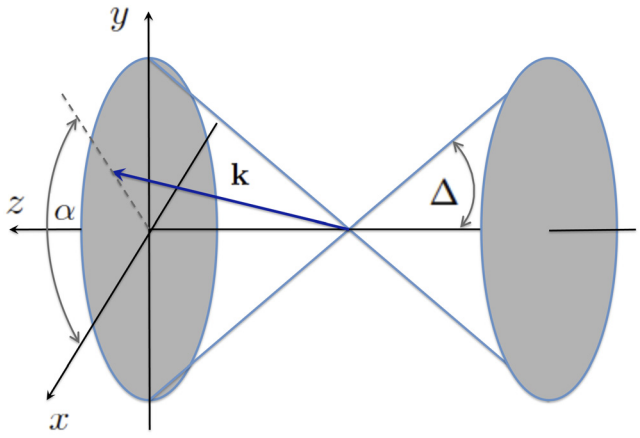

FIG. 1. Schematic illustration of the notation in Eqs. (8)–(11).

$$\nu = \frac{2\pi\Delta}{\lambda}(x\cos\alpha + y\sin\alpha), \qquad \chi = \frac{2\pi\Delta^2}{\lambda}z, \tag{9}$$

and the function G is given by the integral

$$G(\nu,\chi,\Delta) = 2\int_0^1 du\, f_1(u,\Delta)\exp[i\nu f_1(u,\Delta) - i\chi f_2(u,\Delta)], \tag{10}$$

with

$$f_1(u,\Delta) = \frac{\sin\Delta u}{\Delta}, \qquad f_2(u,\Delta) = \frac{2\sin^2(\Delta u/2)}{\Delta^2}. \tag{11}$$

This solution describes a field with its maximum amplitude E_0 at the origin, $\nu = \chi = 0$, and the intensity distribution shown in Fig. 2. To provide a meaningful comparison of the ion yields produced in the two beams, we choose their parameters such that the maximum intensity $\mathcal{I}_m$ and focal volume V calculated for the parabolic expansion near the focus center are respectively equal. These requirements are met if $\mathcal{I}_m$ in Eq. (6) and E_0 in Eq. (8) are connected by Eq. (1) and

$$\Delta = 2^{3/4}\theta. \tag{12}$$

Although the value of $cE_0^2/8\pi$ in Eq. (1) is not the true intensity, it differs from that defined as the absolute value of the Poynting vector only by terms $\sim\Delta \ll 1$. Most of our calculations are done for $\Delta = 0.178$, which corresponds, through Eq. (12), to an interaction volume equal to that of a Gaussian beam with $w_0 = 3$ μm. To test the tight-focusing case, some calculations were also done for $\Delta = 0.35$, which makes the linear size of the focal spot approximately two times smaller. Then, the $1/e^2$ focal diameter is ≈ 2 μm along the y axis and ≈ 4 μm along the x axis [see Fig. 2(b)], which corresponds approximately to the focal spot used in the simulations in Ref. 31 and exceeds that in Ref. 55 by a factor of ≈ 1.5.

Both the solutions in Eqs. (6) and (8) describe monochromatic static beams, while we devise a theory applicable for description of ionization dynamics in femtosecond laser pulses. A time-dependent envelope can be added as a factor. When this is done, the solutions are no longer exact. However, they remain approximately valid under

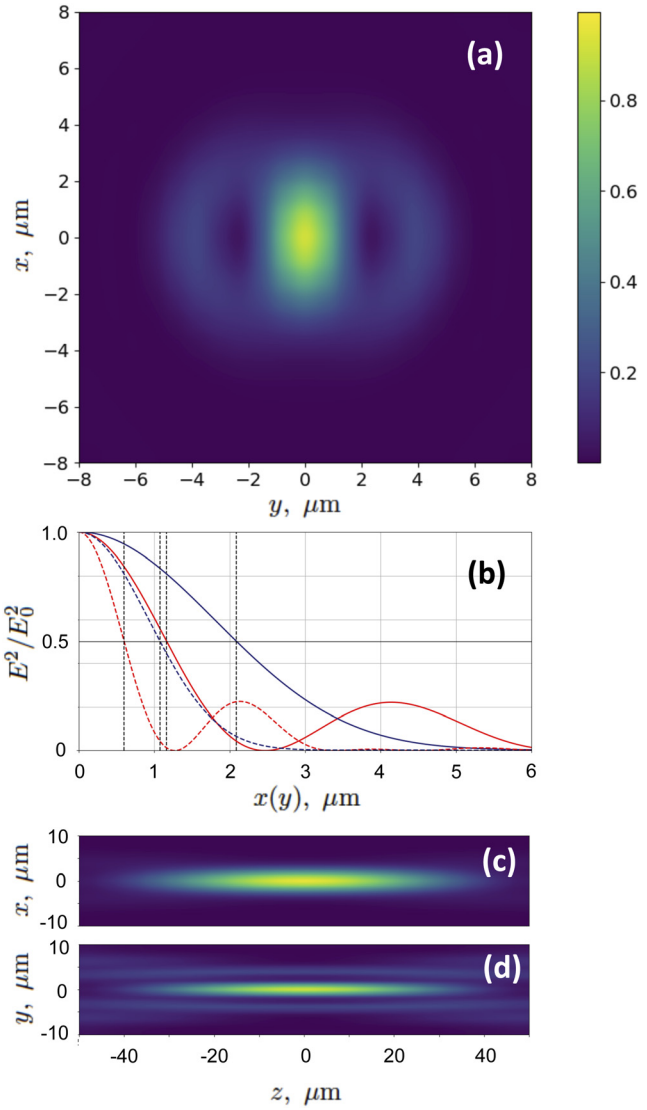

FIG. 2. Normalized distributions of the effective intensity [Eq. (1)] in the planes (x, y, z = 0) (a), (x, y = 0, z) (c), and (x = 0, y, z) (d) for the NF beam with $\Delta = 0.178$ corresponding to the parameters $\lambda = 1$ μm and $w_0 = 3$ μm of the Gaussian beam [Eq. (6)]. (b) shows the cuts $x = 0$ (solid red line) and $y = 0$ (solid blue line) of the (x, y, $z = 0$) distribution in (a). The dashed lines show the analogous cuts for the NF beam with $\Delta = 0.35$.

condition $T \gg w_0/c$, which is reasonably well satisfied for the chosen $w_0 = 3$ μm and $T = 33$ fs.

IV. RESULTS AND DISCUSSION

Using the intensity-dependent populations C_k numerically found in Ref. 23, we calculate the number of highly charged ions of argon, krypton, and xenon in the intensity interval 3×10^{20} W/cm^2–5×10^{24} W/cm^2. The results are shown in Fig. 3. The initial neutral gas density is taken as $n_0 = 2 \times 10^{12}$ cm^{-3}, which corresponds

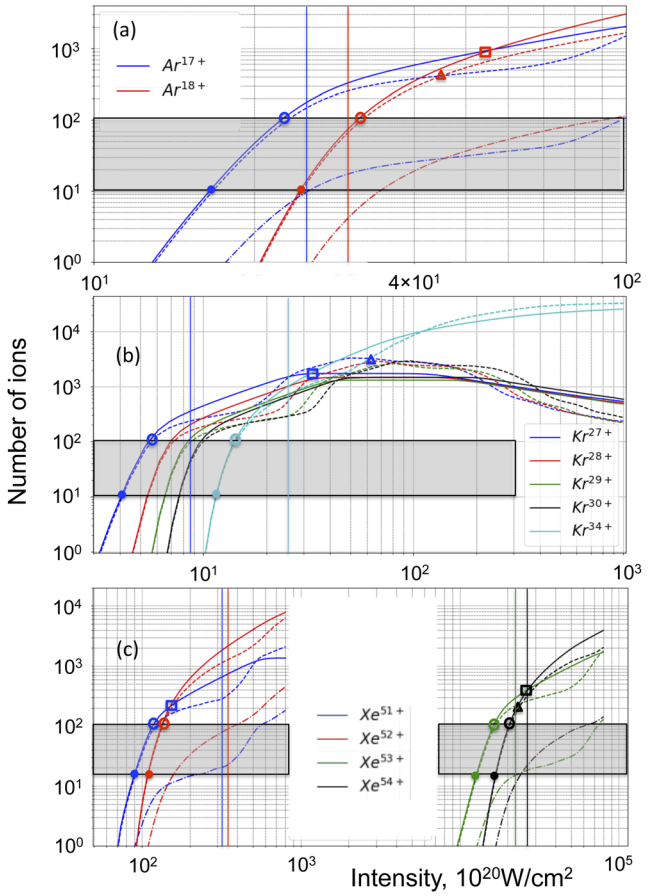

FIG. 3. Number of ions vs peak laser intensity calculated from Eq. (5) for argon (a), krypton (b), and xenon (c) using the intensity distributions for the Gaussian (solid lines) and NF (dashed lines) beams. The beam parameters are the same as in Fig. 2. For argon and for Xe^{51+} and Xe^{52+}, the results corresponding to the tightly focused NF beam with $\Delta = 0.35$ are shown by dash-dotted lines. The gray areas indicate the interval $N(A^{k+}) = 10$–100 where the number of ions grows by one order of magnitude. The values of $\mathcal{I}_{10}$ and $\mathcal{I}_{100}$ given in Table I are indicated by filled and open circles, respectively. The values of $\mathcal{I}_0$ where the numbers of two selected charge states become equal are shown by open squares for the Gaussian beam and by open triangles for the NF beam. For the pair of states Xe^{51+} and Xe^{52+}, the values of $\mathcal{I}_0$ for the two beams are difficult to distinguish visually, and so the corresponding triangle symbol is omitted. Vertical lines indicate the threshold intensities calculated from the analytic estimate in Eq. (13).

to a pressure in the gas jet $\approx 5.6 \times 10^{-5}$ Torr at room temperature. These parameters of the gas target are numerically close to those used in the experiment described in Ref. 22, where the method of atomic diagnostics was verified. In the same experiment, a TOF detector with ≈50% efficiency was used to identify the highest ionic states. For a high-quality detector, it can reasonably be assumed that several dozen ions produced in the central part of the focus will be sufficient for a reliable measurement in the single-shot regime. We set the detection threshold as $N(A^{k+}) \approx 10$. Above this threshold and for the chosen values of n_0 and w_0, the number of ions grows by approximately one order of magnitude in a relatively narrow interval of intensity. We denote the corresponding intensities by $\mathcal{I}_{10}$ and $\mathcal{I}_{100}$. Their numerical values are shown in Table I for the two pulse shapes. For the intervals $\Delta\mathcal{I} = \mathcal{I}_{100} - \mathcal{I}_{10}$ of intensity corresponding to a one order-of-magnitude growth in the number of ions, the data in the table give $\Delta\mathcal{I}(Ar^{18+}) \approx 0.7 \times 10^{21}$ W/cm^2, $\Delta\mathcal{I}(Kr^{34+}) \approx 0.3 \times 10^{21}$ W/cm^2, $\Delta\mathcal{I}(Xe^{52+}) \approx 0.2 \times 10^{22}$ W/cm^2, and $\Delta\mathcal{I}(Xe^{54+}) \approx 0.5 \times 10^{24}$ W/cm^2. These values, along with those of $\mathcal{I}_{10}$ and $\mathcal{I}_{100}$, can be used to determine the peak intensity value with accuracy ≤30% by detecting the highest charge states in discernible amounts. It is instructive to compare the values of $\mathcal{I}_{10}$ and $\mathcal{I}_{100}$ with that introduced in Ref. 23 on the basis of a simple estimate made with logarithmic accuracy [see Eq. (14) there]. This equation can be reformulated as

$$\mathcal{I}_* \approx 7.03 \times 10^{-6} (I_p)^3 [10^{20}] \text{ W/cm}^2. \quad (13)$$

The values of $\mathcal{I}_*$ are given in Table I and are shown in Fig. 3 by vertical red lines. For Ar^{18+}, the estimate from Ref. 23 is in a good agreement with $\mathcal{I}_{100}$, while for the ions of Kr and Xe, a roughly 50% difference is apparent. This discrepancy is, however, not crucial, since the estimate in Eq. (13) is only designed to approximately locate the domain of intensities that can be probed with the given charge state.

It can clearly be seen that the ion yields calculated for the two pulse shapes practically coincide in the domain $N(A^{k+}) = 10$–100, where they can already be reliably detected by a sensitive TOF setup. This makes the approach based on the identification of the intensity interval corresponding to rapid growth in the ion signal within $N \sim 10$–100 practically insensitive to the pulse shape, provided the focal spot diameter is approximately known. A serious drawback of this algorithm stems from the fact that the efficiency of the TOF detector and the atomic concentration n_0 in the gas jet might not be precisely measured. These two uncertainties will lead to an uncertainty in the coefficient connecting the number of ions shown by the curves of Fig. 3 and the number of counts in the TOF detector. Moreover, an uncertainty in the focal diameter of a factor of 2 or more will have a considerable effect on the value of $\mathcal{I}_{10}$ and even more on that of $\mathcal{I}_{100}$. To demonstrate this sensitivity, we calculated the yields of Ar^{17+}, Ar^{18+}, Xe^{51+}, and Xe^{52+} for the NF beam at the same peak amplitude but with a value of Δ twice as large, i.e., $\Delta = 0.35$, which corresponds to a FWHM spot size of $\approx 1.2 \times 2.2$ μm^2. The effective focal volume then appears roughly 16 times smaller than that for $\Delta = 0.178$. As a result, for Xe, the value of $\mathcal{I}_{10}$ increases by ≈30%–40%, while that of $\mathcal{I}_{100}$ increases by several times. The corresponding shifts for Ar are even bigger. Exact values are given in Table I. This observation shows that measurement just of the absolute number of ions might be insufficient for accurate determination of the peak intensity.

A complementary approach can be based on determination of the intensities for which the numbers of two charge states appear equal.[25] These points are indicated in Fig. 3 by open squares (for the Gaussian beam) and open triangles (for the NF beam) for the pairs of charge states Ar^{17+} and Ar^{18+}, Kr^{27+} and Kr^{34+}, Xe^{51+} and Xe^{52+}, and Xe^{53+} and Xe^{54+}. Numerical values of these intensities, denoted by $\mathcal{I}_0$, are given in Table I. The positions of the intersection points do not depend on n_0 or on the detector efficiency, provided the latter is close for the two ions of the chosen charge states. However, these positions do depend on the focal intensity distribution, as can be seen from the data in Fig. 3 and Table I. Moreover, the positions of these intersections remain almost insensitive to the focal spot size, as can be seen by comparing the curves for argon and xenon calculated for two

TABLE I. Reference intensity values for ion yields shown in Fig. 3: $\mathcal{I}_{10}$ and $\mathcal{I}_{100}$ are the intensities corresponding to $N(A^{k+}) = 10$ and $N(A^{k+}) = 100$, respectively, $\mathcal{I}_0$ is the value of intensity such that $N(A^{k+}) = N(A^{(k+1)+})$, and $\mathcal{I}_*$ is given by the analytic estimate in Eq. (13). Intensities are given in units of 10^{20} W/cm^2. The parameters of the laser beams are $w_0 = 3$ μm, $\lambda = 1$ μm, and $\Delta = 0.178$. Values of $\mathcal{I}_{10}$ and $\mathcal{I}_{100}$ for the NF beam with $\Delta = 0.35$ are shown in parentheses for Ar^{17+} and Xe^{52+}.

Ion	I_p (eV)	$\mathcal{I}_{10}^{G}$	$\mathcal{I}_{10}^{NF}$	$\mathcal{I}_{100}^{G}$	$\mathcal{I}_{100}^{NF}$	$\mathcal{I}_{0}^{G}$	$\mathcal{I}_{0}^{NF}$	$\mathcal{I}_*$
Ar^{17+}	4120	17	17 (25)	23	23 (98)	56	45	24
Ar^{18+}	4426	24	25	31	32			30
Kr^{27+}	2929	4.1	4.1	5.5	5.7	32	62	8.8
Kr^{34+}	4108	11	11	14	14			24
Xe^{51+}	9607	86	87	118	120	151	140	310
Xe^{52+}	9812	110	106 (145)	130	130 (381)			330
Xe^{53+}	40 272	1.2×10^4	1.2×10^4	1.6×10^4	1.7×10^4	2.7×10^4	2.5×10^4	2.3×10^4
Xe^{54+}	41 300	1.6×10^4	1.6×10^4	2.1×10^4	2.0×10^4			2.5×10^4

different values of Δ for the NF beam. The greater the difference in the ionization potentials, the further is the intersection point from the initial steep part of the yield curve and the greater is the difference in their positions found for the two beams.

Finally, the value of the intensity can be inferred from the slopes of the ion yields. Figure 4 shows the doubly logarithmic derivative of the ion yield vs laser intensity for argon and xenon. The value of the slope decreases monotonically with increasing intensity (except in the domain of sufficiently high intensities, where the volume effect becomes quite strongly dependent on the intensity distribution) and appears remarkably independent of the spot size and only weakly sensitive to the pulse shape. Note that the intensity distributions in the focal plane appear quite different for the Gaussian and NF beams. Therefore, one may expect that the slope is in general rather weakly sensitive to this distribution, which in practice may appear quite complicated (see, e.g., Refs. 56 and 57). This feature makes the slope probably the most precise measure of the peak intensity. However, as in the case of the yield intersection points, measuring this value requires a set of laser shots at known relative energies, so that the ratio of intensities for subsequent shots can be reliably estimated. This might appear problematic for multi-PW lasers.

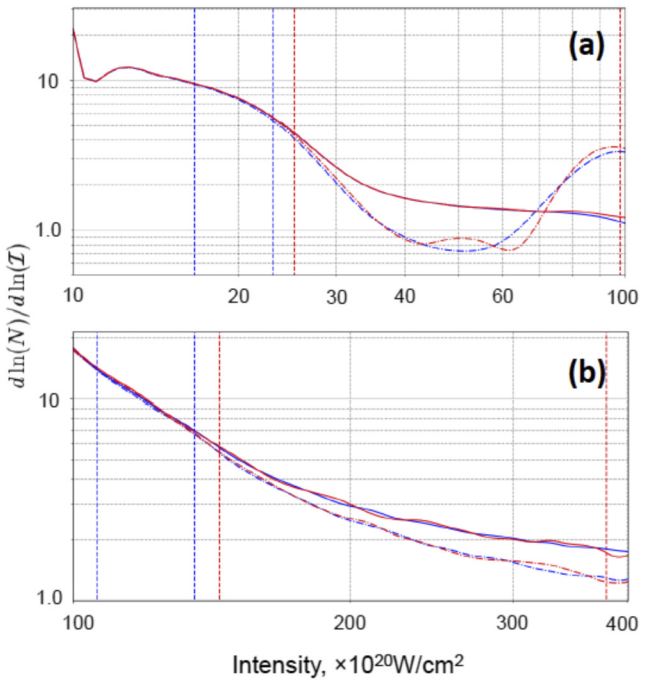

FIG. 4. Derivative $d\log(N)/d\log(\mathcal{I})$ for Ar^{17+} (a) and Xe^{52+} (b) calculated for the parameters of Fig. 3. Solid curves correspond to the Gaussian beam and dash-dotted curves to the NF beam. $\Delta = 0.178$ for the blue curves and $\Delta = 0.35$ for the red curves.

V. CONCLUSIONS

In conclusion, we studied the effect of the focal intensity distribution on the method of peak intensity determination based on the observation of multiple tunneling ionization of heavy atoms. Three algorithms for extraction of the peak intensity value were examined. The first, based on the detection of new charge states that appear as the intensity increases, was shown to be essentially shape-independent in the intensity interval where this number grows quickly. It suffers from some uncertainty resulting from the uncertainties in the TOF detection efficiency, the atomic concentration in the gas jet, and, most of all, in the focal spot size. The second algorithm requires measurement of the ratio of the ion numbers for two selected charge states. It is robust with respect to the TOF efficiency, atomic concentration, and focal spot size, but appears in general to be dependent on the intensity distribution in the focal spot. This dependence is less pronounced for pairs of charge states with relatively close ionization potentials, such as the pair Xe^{51+} and Xe^{52+} and the pair Xe^{53+} and Xe^{54+}. Finally, the third algorithm relies on measurement of the slope of the intensity dependence of the ion yield. In the interval of intensities where this slope is high, ≈5–10, the algorithm appears essentially insensitive to the factors discussed above, including the intensity distribution within the focal spot. The second and third algorithms do, however, require multiple consecutive measurements with controllable relative laser pulse energies, which could be challenging for lasers of extreme power. In an experiment targeted to measure the peak intensity value through the detection of highly charged ions produced in the process of tunneling ionization, the three algorithms can be simultaneously applied to increase the accuracy.

We also presented a brief comparative overview of several approaches for *in situ* measurement of extreme laser intensities.

We hope that our analysis will help to provide the reader with some orientation in this currently emerging field of laser diagnostics. The present paper concludes a set of publications[23–25] dedicated to theoretical analysis of the atomic diagnostics method for extreme laser intensities.

ACKNOWLEDGMENTS

The authors are grateful to S. V. Bulanov, A. Fedotov, G. Korn, E. Khazanov, A. Soloviev, and S. Weber for stimulating discussions and useful suggestions. S.V.P. acknowledges financial support from the Russian Foundation for Basic Research via Grant No. 19-02-00643. M.F.C. acknowledges the Spanish Ministry MINECO and State Research Agency AEI (FIDEUA PID2019-106901GB-I00/10.13039/501100011033, SEVERO OCHOA No. SEV-2015-0522, FPI), European Social Fund, Fundació Cellex, Fundació Mir-Puig, Generalitat de Catalunya (AGAUR Grant No. 2017 SGR 1341, CERCA program, QuantumCAT U16-011424, co-funded by ERDF Operational Program of Catalonia 2014-2020), MINECO-EU QUANTERA MAQS (funded by The State Research Agency (AEI) PCI2019-111828-2/10.13039/501100011033), the National Science Centre, Poland-Symfonia Grant No. 2016/20/W/ST4/00314 and the project Advanced Research Using High Intensity Laser Produced Photons and Particles (Grant No. CZ.02.1.01/0.0/0.0/16_019/0000789) through the European Regional Development Fund (ADONIS).

REFERENCES

[1]F. Krausz and M. Ivanov, "Attosecond physics," Rev. Mod. Phys. **81**, 163 (2009).
[2]L. F. DiMauro and P. Agostini, "Atomic and molecular ionization dynamics in strong laser fields: From optical to X-rays," Adv. At., Mol., Opt. Phys. **61**, 117 (2012).
[3]B. M. Karnakov, V. D. Mur, S. V. Popruzhenko *et al.*, "Current progress in developing the nonlinear ionization theory of atoms and ions," Phys.-Usp. **58**, 3 (2015).
[4]G. Mourou, T. Tajima, and S. V. Bulanov, "Optics in the relativistic regime," Rev. Mod. Phys. **78**, 309 (2009).
[5]A. Di Piazza, C. Müller, K. Z. Hatsagortsyan *et al.*, "Extremely high-intensity laser interactions with fundamental quantum systems," Rev. Mod. Phys. **84**, 1177 (2012).
[6]N. B. Narozhny and A. M. Fedotov, "Extreme light physics," Contemp. Phys. **56**, 249 (2015).
[7]M. D. Perry, D. Pennington, B. C. Stuart *et al.*, "Petawatt laser pulses," Opt. Lett. **24**, 160 (1999).
[8]S.-W. Bahk, P. Rousseau, T. A. Planchon *et al.*, "Generation and characterization of the highest laser intensities (10^{22} W/cm^2)," Opt. Lett. **29**, 2837 (2004).
[9]V. Yanovsky, V. Chvykov, G. Kalinchenko *et al.*, "Ultra-high intensity 300-TW laser at 0.1 Hz repetition rate," Opt. Express **16**, 2109 (2008).
[10]Z. Guo, L. Yu, J. Wang *et al.*, "Improvement of the focusing ability by double deformable mirrors for 10-PW-level Ti:sapphire chirped pulse amplification laser system," Opt. Exp. **26**, 26776 (2018).
[11]D. N. Papadopoulos, J. P. Zou, C. Le Blanc *et al.*, "The Apollon 10 PW laser: Experimental and theoretical investigation of the temporal characteristics," High Power Laser Sci. Eng. **4**, E34 (2016); "First commissioning results of the Apollon laser on the 1 PW beam line," in Conference on Lasers and Electro-Optics (CLEO), 2019.
[12]J. H. Sung, H. W. Lee, J. Y. Yoo *et al.*, "4.2 PW, 20 fs Ti:sapphire laser at 0.1 Hz," Opt. Lett. **42**, 2058 (2017).
[13]X. Zeng, K. Zhou, Y. Zuo *et al.*, "Multi-petawatt laser facility fully based on optical parametric chirped-pulse amplification," Opt. Lett. **42**, 2014 (2017).
[14]Z. Gan, L. Yu, S. Li *et al.*, "200 J high efficiency Ti:sapphire chirped pulse amplifier pumped by temporal dual-pulse," Opt. Exp. **25**, 5169 (2017); W. Li, Z. Gan, L. Yu *et al.*, "339 J high-energy Ti:sapphire chirped-pulse amplifier for 10 PW laser facility," Opt. Lett. **43**, 5681 (2018).
[15]J.-P. Chambaret, O. Chekhlov, G. Cheriaux *et al.*, "Extreme light infrastructure: Laser architecture and major challenges," Proc. SPIE **7721**, 77211D (2010).
[16]S. Weber, S. Bechet, S. Borneiset *et al.*, "P3: An installation for high-energy density plasma physics and ultra-high intensity laser–matter interaction at ELI-beamlines," Matter Radiat. Extremes **2**, 149 (2017).
[17]A. V. Bashinov, A. A. Gonoskov, A. V. Kim *et al.*, "New horizons for extreme light physics with mega-science project XCELS," Eur. Phys. J.: Spec. Top. **223**, 1105 (2014).
[18]C. A. Chowdhury, C. P. J. Barty, and B. C. Walker, ""Nonrelativistic" ionization of the L-shell states in argon by a "relativistic" 10^{19} W/cm^2 laser field," Phys. Rev. A **63**, 042712 (2001).
[19]E. A. Chowdhury and B. C. Walker, "Multielectron ionization processes in ultrastrong laser fields," J. Opt. Soc. Am. B **20**, 109 (2003).
[20]K. Yamakawa, Y. Akahane, Y. Fukuda *et al.*, "Ionization of many-electron atoms by ultrafast laser pulses with peak intensities greater than 10^{19} W/cm^2," Phys. Rev. A **68**, 065403 (2003).
[21]K. Yamakawa, Y. Akahane, Y. Fukuda *et al.*, "Super strong field ionization of atoms by 10^{19} W/cm^2, 10 Hz laser pulses," J. Mod. Opt. **50**, 2515 (2003).
[22]A. Link, E. A. Chowdhury, J. T. Morrison *et al.*, "Development of an *in situ* peak intensity measurement method for ultraintense single shot laser-plasma experiments at the Sandia Z petawatt facility," Rev. Sci. Instrum. **77**, 10E723 (2006).
[23]M. F. Ciappina, S. V. Popruzhenko, S. V. Bulanov *et al.*, "Progress toward atomic diagnostics of ultrahigh laser intensities," Phys. Rev. A **99**, 043405 (2019).
[24]M. F. Ciappina, S. V. Bulanov, T. Ditmire *et al.*, "Towards laser intensity calibration using high-field ionization," in *Progress in Ultrafast Intense Laser Science XV*, Topics in Applied Physics Vol. 136, edited by K. Yamanouchi and D. Charalambidis (Springer Nature, Switzerland, 2020) (in press).
[25]M. F. Ciappina and S. V. Popruzhenko, "Diagnostics of ultra-intense laser pulses using tunneling ionization," Laser Phys. Lett. **17**, 025301 (2020).
[26]O. Har-Shemesh and A. Di Piazza, "Peak intensity measurement of relativistic lasers via nonlinear Thomson scattering," Opt. Lett. **37**, 1352 (2012).
[27]C. Z. He, A. Longman, J. A. Pérez-Hernández *et al.*, "Towards an in situ, full-power gauge of the focal-volume intensity of petawatt-class lasers," Opt. Exp. **27**, 30020 (2019).
[28]T. G. Blackburn, E. Gerstmayr, S. P. D. Mangles *et al.*, "Model-independent inference of laser intensity," Phys. Rev. Acc. Beams. **23**, 064001 (2020).
[29]F. Mackenroth, A. R. Holkundkar, and H.-P. Schlenvoigt, "Ultra-intense laser pulse characterization using ponderomotive electron scattering," New J. Phys. **21**, 123028 (2019).
[30]O. E. Vais, A. G. R. Thomas, A. M. Maksimchuk *et al.*, "Characterizing extreme laser intensities by ponderomotive acceleration of protons from rarified gas," New J. Phys. **22**, 023003 (2020).
[31]A. Yandow, T. Toncian, and T. Ditmire, "Direct laser ion acceleration and above-threshold ionization at intensities from 10^{21} W/cm^2 to 3×10^{23} W/cm^2," Phys. Rev. A **100**, 053406 (2019).
[32]J. R. Oppenheimer, "Three notes on the quantum theory of aperiodic effects," Phys. Rev. **31**, 66 (1928).
[33]N. B. Narozhny and M. S. Fofanov, "Scattering of relativistic electrons by a focused laser pulse," J. Exp. Theor. Phys. **90**, 753 (2000).
[34]A. I. Nikishov and V. I. Ritus, "Quantum processes in the field of a plane electromagnetic wave and in a constant field. I," Zh. Eksp. Teor. Fiz. **46**, 776 (1964) [Sov. Phys. JETP **19**, 529 (1964) (in English)].
[35]V. B. Berestetskii, E. M. Lifshitz, and L. P. Pitaevskii, *Quantum Electrodynamics* (Butterworth-Heinemann, 1982), Chap. IV, Sec. 101, ISBN: 978-0-7506-3371-0.
[36]E. S. Sarachik and G. T. Schappert, "Classical theory of the scattering of intense laser radiation by free electrons," Phys. Rev. D **1**, 2738 (1970).
[37]O. E. Vais and V. Yu. Bychenkov, "Direct electron acceleration for diagnostics of a laser pulse focused by an off-axis parabolic mirror," Appl. Phys. B **124**, 211 (2018).
[38]T. W. B. Kibble, "Mutual refraction of electrons and photons," Phys. Rev. **150**, 1060 (1966).
[39]S. P. Goreslavsky, N. B. Narozhny, and V. P. Yakovlev, "Electron spectra of above-threshold ionization in a spatially inhomogeneous field," J. Opt. Soc. Am. B **6**, 1752

(1989); S. P. Goreslavsky and N. B. Narozhny, "Ponderomotive scattering at relativistic laser intensities," J. Nonlinear Opt. Phys. Matter **04**, 799 (1995).

[40]D. B. Milosević, G. G. Paulus, D. Bauer *et al.*, "Above-threshold ionization by few-cycle pulses," J. Phys. B: At., Mol. Opt. Phys. **39**, R203 (2006).

[41]S. V. Popruzhenko, "Keldysh theory of strong field ionization: History, applications, difficulties and perspectives," J. Phys. B: At., Mol. Opt. Phys. **47**, 204001 (2014).

[42]W. Becker, S. P. Goreslavski, D. B. Miloñević *et al.*, "The plateau in above-threshold ionization: The keystone of rescattering physics," J. Phys. B: At., Mol. Opt. Phys. **51**, 162002 (2018).

[43]M. Kübel, M. Arbeiter, C. Burger *et al.*, "Phase- and intensity-resolved measurements of above threshold ionization by few-cycle pulses," J. Phys. B: At., Mol. Opt. Phys. **51**, 134007 (2018).

[44]V. V. Strelkov, E. Mével, and E. Constant, "Short pulse carrier-envelope phase absolute single-shot measurement by photoionization of gases with a guided laser beam," Opt. Exp. **22**, 6239 (2014).

[45]M. G. Pullen, W. C. Wallace, D. E. Laban *et al.*, "Measurement of laser intensities approaching 10^{15} W/cm^2 with an accuracy of 1%," Phys. Rev. A **87**, 053411 (2013).

[46]L. V. Keldysh, "Ionization in the field of a strong electromagnetic wave," J. Exp. Theor. Phys. **47**, 1945 (1964) [Sov. Phys. JETP **20**, 1307 (1965) (in English)].

[47]A. M. Perelomov, V. S. Popov and M. V. Terentev, "Ionization of atoms in an alternating electric field. I," J. Exp. Theor. Phys. **50**, 1393 (1966) [Sov. Phys. JETP **23**, 924 (1966) (in English)].

[48]A. M. Perelomov and V. S. Popov, "Ionization of atoms in an alternating electric field. III," J. Exp. Theor. Phys. **52**, 514 (1967) [Sov. Phys. JETP **25**, 336 (1967) (in English)].

[49]V. S. Popov, "Tunnel and multiphoton ionization of atoms and ions in a strong laser field (Keldysh theory)," Usp. Fiz. Nauk **174**, 921 (2004) [Phys.-Usp. **47**, 855 (2004) (in English)].

[50]X. M. Tong and C. D. Lin, "Empirical formula for static field ionization rates of atoms and molecules by lasers in the barrier-suppression regime," J. Phys. B: At., Mol. Opt. Phys. **38**, 2593 (2005).

[51]I. Yu. Kostyukov and A. A. Golovanov, "Field ionization in short and extremely intense laser pulses," Phys. Rev. A **98**, 043407 (2018).

[52]E. B. Saloman, "Energy levels and observed spectral lines of ionized argon, Ar II through Ar XVIII," J. Phys. Chem. Ref. Data **39**, 033101 (2010).

[53]E. B. Saloman, "Energy levels and observed spectral lines of krypton, Kr I through Kr XXXVI," J. Phys. Chem. Ref. Data **36**, 215 (2007).

[54]E. B. Saloman, "Energy levels and observed spectral lines of xenon, Xe I through Xe LIV," J. Phys. Chem. Ref. Data **33**, 765 (2004).

[55]E. A. Chowdhury, I. Ghebregziabher, J. Macdonald *et al.*, "Electron momentum states and bremsstrahlung radiation from the ultraintense field ionization of atoms," Opt. Express **12**, 3911 (2004).

[56]G. Pariente, V. Gallet, A. Borot *et al.*, "Space-time characterization of ultra-intense femtosecond laser beams," Nat. Photonics **10**, 547 (2016).

[57]A. Jeandet, A. Borot, K. Nakamura *et al.*, "Spatio-temporal structure of a petawatt femtosecond laser beam," J. Phys.: Photonics **1**, 035001 (2019).